Available online at www.sciencedirect.com
ScienceDirect
Trans. Nonferrous Met. Soc. China 29(2019) 2331−2339
Transactions of Nonferrous Metals Society of China
www.tnmsc.cn

Modifying element diffusion pathway by transition layer structure in high-entropy alloy particle reinforced Cu matrix composites

Hao-yang YU[1], Wei FANG[1,2], Ruo-bin CHANG[1], Pu-guang JI[1], Qing-zhou WANG[1]

1. Research Institute for Energy Equipment Materials, School of Materials Science and Engineering, Hebei University of Technology, Tianjin 300132, China;
2. Tianjin Key Laboratory of Materials Laminating Fabrication and Interface Control Technology, Tianjin 300132, China

Received 13 January 2019; accepted 3 July 2019

Abstract: The $Al_{0.3}CoCrFeNi$ high-entropy alloy (HEA) particles reinforced Cu matrix composites (CMCs) were fabricated by mechanical alloying and sintering. Transition layer structure was obtained by multi-step ball milling to investigate the related influence on element diffusion behavior and wear properties of CMCs. The results indicate that a new Cu transition layer is generated, and the thickness is about 5 μm. Cr element diffuses into the interface via the transition layer, which forms the complex oxide. Because of the structure of Cu transition layer, the diffusion rates of Ni, Co and Fe increase, especially the Ni element. The wear resistance of CMCs is improved by 30%, which is due to the improvement of interface bonding strength, compared with the CMCs without transition layer. This method is applicable to the development of advanced HEA reinforced metallic matrix composites.
Key words: high-entropy alloy; copper-matrix composites; transition layer structure; diffusion; wear

1 Introduction

Particles reinforced metal-matrix composites (MMCs) have been extensively studied in past decades [1−3]. Carbon nano-tubes [4,5], MoS_2 [6], TiB_2 [7] and SiC [8,9] ceramics are usually chosen as the reinforced phases in MMCs to improve the strength, hardness and wear resistance. However, the differences of expansion coefficient and elastic modulus between matrix and ceramics result in the weak interfacial bonding [8], which limits the application of MMCs. Seeking new type of reinforced phase is a promising way to improve the interfacial bonding strength [10,11].

The high-entropy alloys (HEAs) have received significant attention recently owing to their multiple principle elements, which are a breakthrough of one or two prevalent base elements of conventional alloys [12−14]. Generally, the concentrations of the principal elements are in equal-molar ratios or near equal-molar ratios [12]. There are numerous opportunities for investigations in the huge unexplored compositional space of multicomponent alloys [13]. Different atom sizes of principal elements result in the lattice distortion effect and sluggish diffusion effects, which is positive to obtain high melting point, hardness and strength [15,16]. Compared with the reinforcement phase of ceramic, the metallic character of high-entropy alloy is beneficial to improving the interfacial strength of MMCs.

Several studies have reported that high-entropy alloy particles are selected as reinforced phase of MMCs [17−19]. Interfacial bonding between particles and interface during the sintering process is a prior issue. AlCoCrFeNi high-entropy alloy reinforced Cu matrix composites were fabricated by mechanical alloying and sintering process, and no intermetallic phases are present at the interfaces [17]. However, stress concentration is prone to occur at the interface between matrix and high-entropy alloy particles [18,19], which weakens the properties of MMCs.

Foundation item: Projects (51701061, 51705129) supported by the National Natural Science Foundation of China; Project (17391001D) supported by the Department of Science and Technology of Hebei Province, China; Project (2017-Z02) supported by the State Key Lab of Advanced Metals and Materials, China
Corresponding author: Wei FANG, Tel: +86-22-60204051, E-mail: fangwei@hebut.edu.cn;
Pu-guang JI, Tel: +86-22-60202991, E-mail: jipuguang@hebut.edu.cn
DOI: 10.1016/S1003-6326(19)65139-3

Transition layer structure is considered to effectively improve the wettability, and enhance interfacial strength and mechanical properties of composites [20−22]. Due to high Vickers hardness and single face-centered-cubic structure [23], the $Al_{0.3}CoCrFeNi$ HEA particles were chosen as reinforced phase in this work. Transition layer structure was obtained by multi-step ball milling to investigate the related influence on element diffusion behavior and wear properties of CMCs. It is helpful and inspiring for the development of advanced HEA reinforced metallic matrix composites.

2 Experimental

The $Al_{0.3}CoCrFeNi$ HEA powders were prepared with elemental powders of Al, Co, Cr, Fe and Ni (purity >99.7 wt.% and particle size ≤45 μm) in a high-energy planetary ball milling. Firstly, elemental powders were placed in stainless steel vials with tungsten carbide balls. The ball-to-powder mass ratio was 10:1, and a high purity argon atmosphere was applied during the whole mechanical alloying (MA) process. Then, the powders were subjected to 48 h dry milling at 350 r/min. Thirdly, in order to obtain the coated layer, elemental powder of Cu (purity >99.7 wt.%, particle size ≤45 μm and mass ratio of Cu to $Al_{0.3}CoCrFeNi$ was 1:1) was subsequently placed in vials, and the mixed powders were subjected to 8 h dry milling at 200 r/min, referred to as $M/Al_{0.3}CoCrFeNi$.

The mixture of pure Cu powders and 5 wt.% $M/Al_{0.3}CoCrFeNi$ HEA powders was milled for 2 h under the protection of an argon atmosphere at a rotation speed of 100 r/min. The mixed powders were sintered at 950 °C for 30 min in a vacuum electrical resistance furnace. Similarly, the mixture of Cu powders and 5 wt.% $Al_{0.3}CoCrFeNi$ powders was also sintered by the same method for comparison.

Powder samples with a mass of 40 mg were prepared for DTG analysis (TA 2000). The DTG experiment temperature was raised to 1200 °C under an argon atmosphere at a heating rate of 10 °C/min. X-ray diffraction (XRD) measurements were performed using Bruker D8 DISCOVER equipped with Cu K_α radiation operating at 40 kV and 40 mA, 2θ values between 30° and 110° with a step size 3 (°)/min. The Vickers hardness was measured using a HMV−2T Vickers microhardness tester, and a load of 490 N was applied for 15 s.

Wear behavior was examined using a block-on-ring wear-testing machine (M−200) under the dry sliding condition. The wear specimens were cube with dimensions of 10 mm × 10 mm × 10 mm. Each specimen was fixed in a holder to wear against a 42-mm-diameter GCr15 steel ring with a hardness value of HRC 60. The sliding velocity and time were 200 r/min and 30 min, respectively, with a normal load of 200 N. The composition, line distribution and elements mapping of micro area were obtained using JEOL 8530F electron probe microanalysis (EPMA) measurements. The microstructure of sample was examined with a JEOL 7100F scanning electron microscope (SEM). The specimens for microstructural observation were mechanically polished by using 400−3000 grit sized fine sand papers and diamond pastes to achieve a mirror-like surface finish.

3 Results

3.1 Preparation of HEA particles with copper coating

HEA particles reinforced Cu matrix composites (CMCs) with or without the transition layer structure are prepared by mechanical alloying and sintering process, as shown in Fig. 1. Firstly, the HEA particles are prepared by mechanical alloying for 48 h, and face-

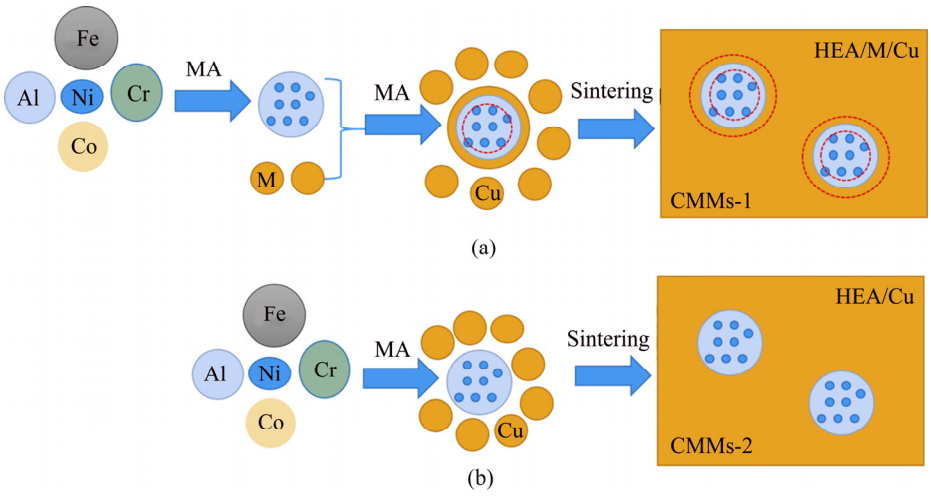

Fig. 1 Schematic diagrams of HEA particles reinforced Cu matrix composites (CMCs) with (a) and without (b) transition layer structure, prepared by mechanical alloying and sintering process (MA: Mechanical alloy; M: Transition layer elements such as Cu)

centered cubic (FCC) phase is evident, as shown in Fig. 2. Then, M powder (M represents transition layer elements such as Cu) is milled with obtained HEA particles, in order to obtain HEA particles coated by Cu layer. Thirdly, the mixture of Cu powder and M/HEA particles is sintered to prepare the CMCs. The CMCs without transition layer are prepared with the Cu powder and HEA particles for comparison. In order to investigate the copper coating on HEA particles by MA, the copper elemental mapping images of Cu and M/HEA powders milled for different time are shown in Fig. 3. The results indicate Cu is uniformly coated on HEA particles after milling for 8 h, referred to as M/HEA particles. As shown in Fig. 2, M/HEA particles exhibit two kinds of FCC phases, corresponding to the phase of Cu and HEA particles. Figure 4 shows the SEM images of Cu, HEA and M/HEA powders, respectively. The sizes of M/HEA particles are 10−30 μm.

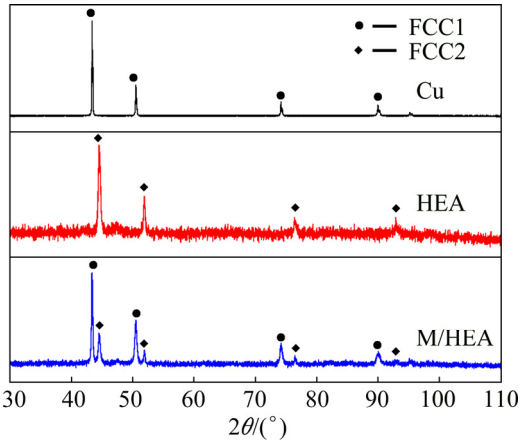

Fig. 2 XRD patterns of Cu, HEA and M/HEA powders

3.2 Diffusion behavior of CMCs during sintering

The M/HEA particles and Cu powders were sintered to obtain HEA/M/Cu composites. For comparison, the mixture of HEA particles and Cu powders was sintered to obtain HEA/Cu composites. The SEM images of the sintered composites are shown in Fig. 5. In order to investigate the stability of HEAs particles during the sintering process, elemental mapping images of HEA/Cu and HEA/M/Cu composites are detected by EPMA, as shown in Fig. 6. The elemental line distributions of HEA/Cu and HEA/M/Cu composites near the interface are shown in Fig. 7. In the HEA/Cu composite, component elements of HEA particles are evenly

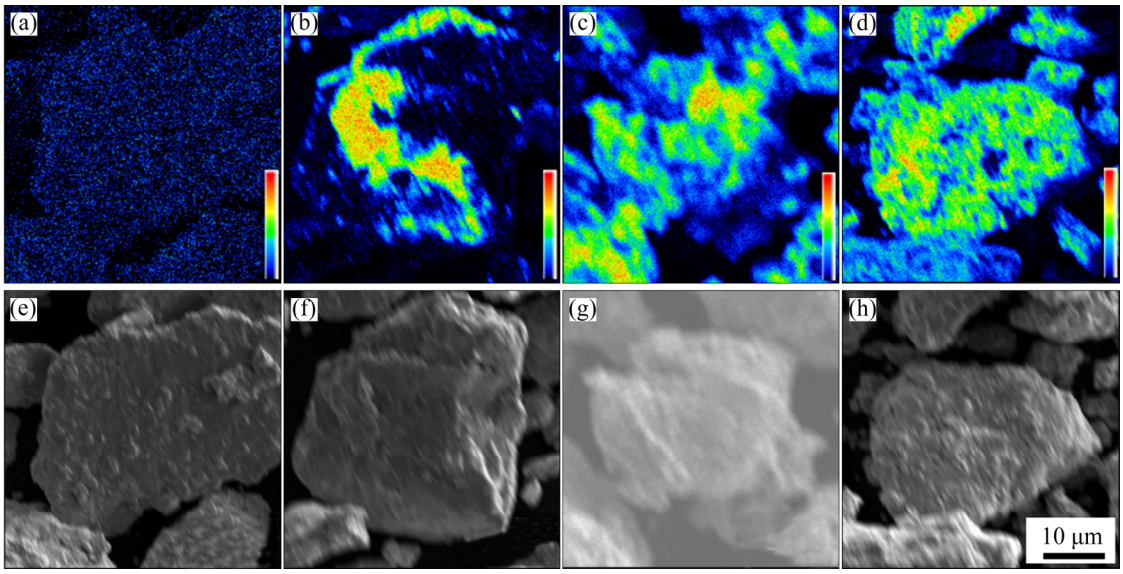

Fig. 3 Elemental mapping images of Cu (a−d) and SEM images of M/HEA powders (e−h) milled for different time: (a, e) 0 h; (b, f) 1 h; (c, g) 4 h; (d, h) 8 h

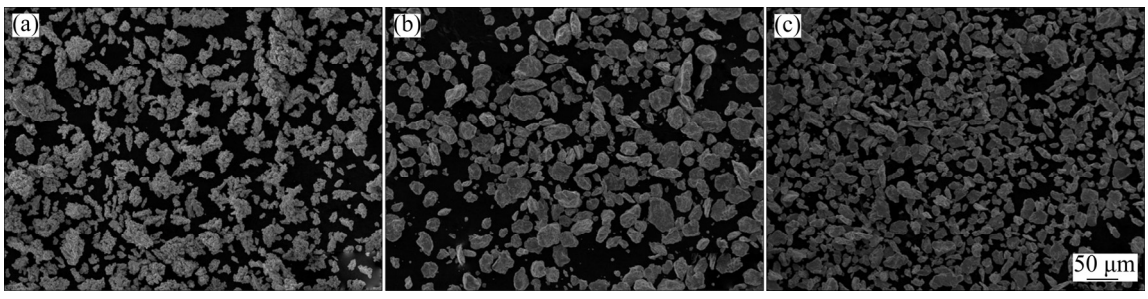

Fig. 4 SEM images of Cu (a), HEA (b) and M/HEA (c) powders

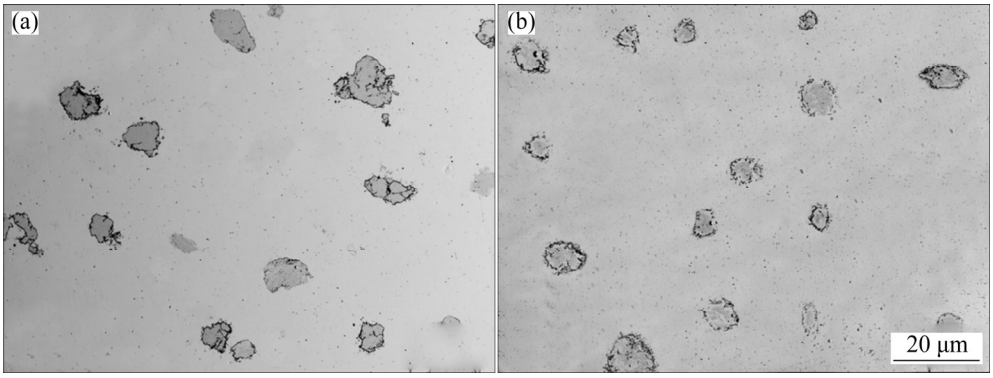

Fig. 5 SEM images of sintered composites: (a) HEA/Cu; (b) HEA/M/Cu

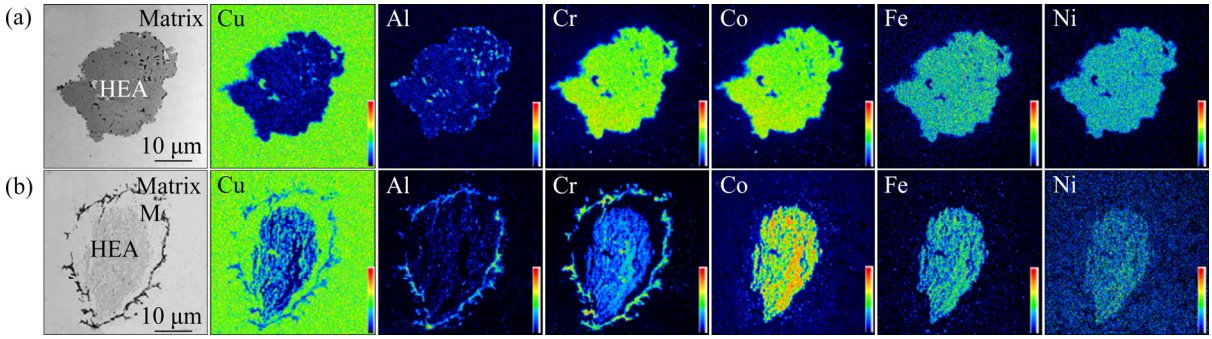

Fig. 6 Elemental mapping images of HEA/Cu (a) and HEA/M/Cu (b) composites by EPMA

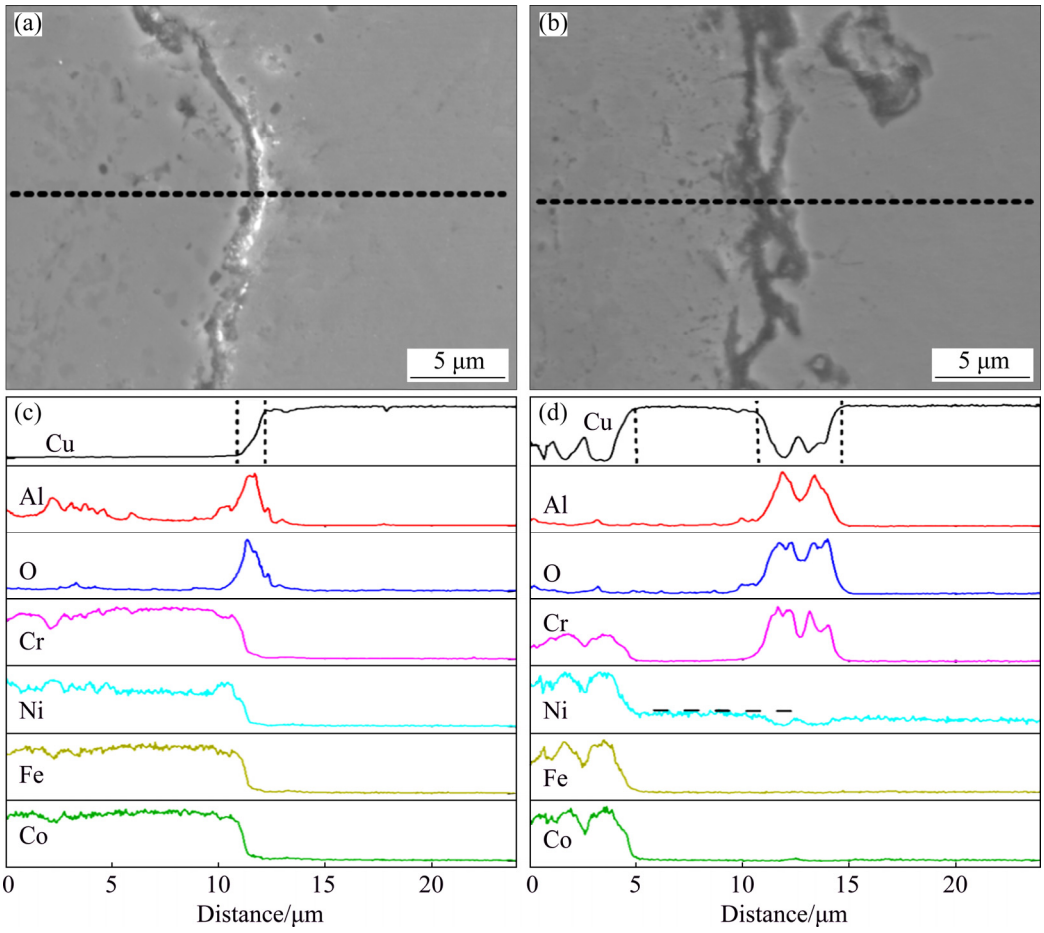

Fig. 7 EPMA line distributions of HEA/Cu (a, c) and HEA/M/Cu (b, d) composites at interface

distributed, and there is an obvious interface between the matrix and HEA particles, according to the mapping image and line distribution results. The element Al is an exception, which is rich at the interface, as shown in Fig. 7(c). However, in the HEA/M/Cu composites, there is a transition layer structure with a thickness of about 5 μm, as shown in Fig. 7(d). Cu is the main element of the transition layer, which is the element of the coated layer on the HEA particles during mechanical alloying. The diffusion behavior of Al and Cr elements is special, which diffuse outwards through the transition layer structure, and rich at the interface. Element mapping images show that Co, Fe and Ni are mainly distributed in the HEA particles, as shown in Fig. 6(b). The intensity of Co and Fe elements maintains equivalent level in the two composites, which indicates that the diffusion of Co and Fe element is sluggish. Few Cu elements gradually diffuse into the HEA particles. The content of Ni in the transition layer is between that of HEA particles and matrix, according to the elemental line distribution in Fig. 7(d). Compared with the Ni distribution of HEA/Cu composites in Fig. 7(c), the diffusion rate of Ni increases owing to the structure of Cu transition layer. The thickness values of the interface in the HEA/Cu and HEA/M/Cu composites are about 1 and 3 μm, respectively. The results indicate that the transition layer changes the diffusion behavior of elements during sintering.

To clarify the detailed distribution of Al and Cr elements, the mapping images at the interface of HEA/Cu and HEA/M/Cu composites are displayed in Fig. 8. The interface of matrix and HEA particles is obvious in the HEA/Cu composites. Al and O elements are mainly concentrated at the interface. These results indicate that Al element diffuses towards the matrix and the oxide forms during the sintering. According to the quantitative analysis results, it is inferred as Al_2O_3. Different from the HEA/Cu composites, Cr element is rich at the interface of HEA/M/Cu composites, and $(Al,Cr)_2O_3$ is inferred to obtain during the sintering.

DTG experiments of HEA/Cu and HEA/M/Cu composites are carried out and the curves during heating are presented in Fig. 9. The peak of HEA/M/Cu composite indicates that a more dramatic chemical reaction occurs, perhaps more Al and Cr elements are transformed near the surface due to the oxygen contamination. As shown in Fig. 10, the hardness of HEA/M/Cu composite is higher than that of HEA/Cu composite, resulting from the solution hardening of Co, Fe and Ni in matrix, as displayed in Table 1. The hardness of HEA particle in HEA/M/Cu is lower than that in HEA/Cu, which is due to the diffusion of Cr element towards the interface.

3.3 Tribological behavior

SEM micrographs of the worn surfaces of the two composites are shown in Figs. 11(a) and (b). The results reveal that the sign and appearance of many grooves and adhesion phenomena are observed in the two composites. In the wear process, the grooves are generated from the surface by the plough of HEA particles. The grooves of HEA/Cu composites are deeper, and more serious shedding phenomena occur, as shown in Fig. 11(a). The results indicate that the HEA particles are better combined with the matrix in HEA/M/Cu composites. The wear rates of HEA/Cu and HEA/M/Cu composites are shown in Fig. 11(c). HEA/M/Cu composites have a better wear resistance than HEA/Cu composites (about 30% increment). A significantly higher wear resistance than that of HEA/Cu composites is attributable to the improvement of interface bonding strength.

The schematic diagrams of the effect of transition layer structure on elemental diffusion during sintering are shown in Fig. 12. According to the experimental results, the pathway of elemental diffusion during sintering is modified via the transition layer structure fabricated by mechanical alloying. Owing to the transition layer structure, more Cr elements are diffused into the interface, which form the complex oxide. More Ni elements are diffused into the matrix via the transition

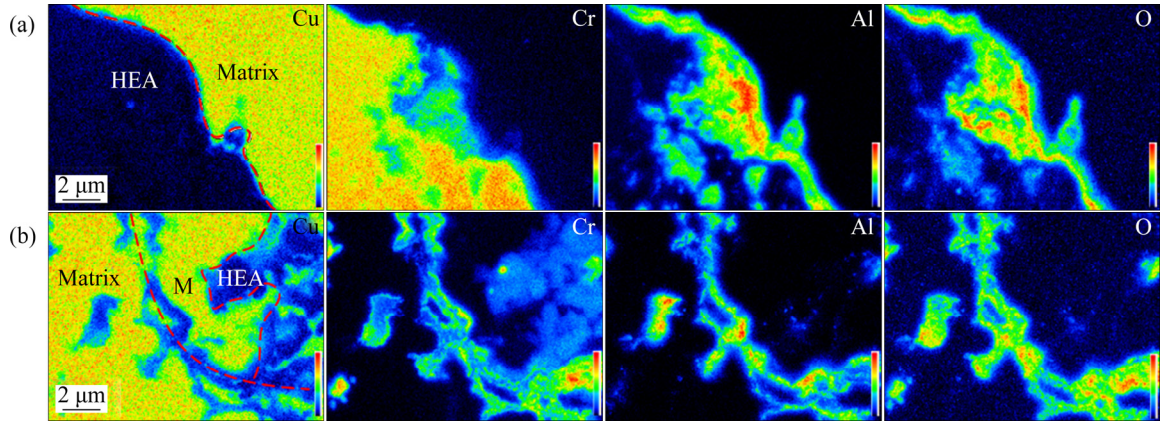

Fig. 8 Elemental mapping images of HEA/Cu (a) and HEA/M/Cu (b) composites at interface by EPMA

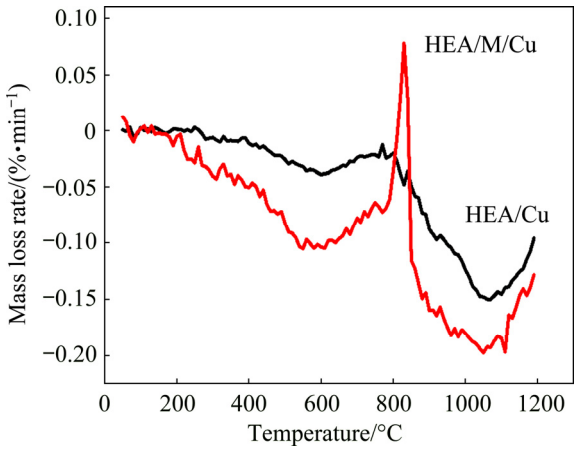

Fig. 9 DTG curves of HEA/Cu and HEA/M/Cu composites

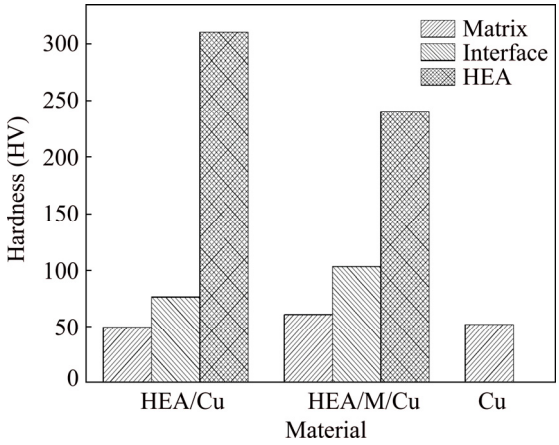

Fig. 10 Hardness distributions of HEA/Cu and HEA/M/Cu composites

Table 1 Chemical compositions of matrix, particles and interfaces in two composites measured by EPMA

Composite	Region	Content/at.%						
		Al	Co	Cr	Fe	Ni	O	Cu
HEA/Cu	HEA	6.7	23.2	23.9	20.3	19.6	0.2	6.1
	Interface	35.6	0.1	0.2	0.2	0.1	51.5	12.3
	Cu matrix	0.3	0.2	0.2	0.2	0.2	1.8	97.1
HEA/M/Cu	HEA	2.2	33.7	18.5	30.8	8.4	0.0	6.4
	Interface	28.5	0.6	10.0	0.7	0.4	49.4	10.4
	Cu matrix	0.2	0.6	0.1	0.6	1.0	1.8	95.7

layer. The diffusion behavior changes the hardness and improves the wear resistance of HEA reinforced Cu matrix composites. This method is potential and applicable for the development of advanced HEA reinforce metallic matrix composites.

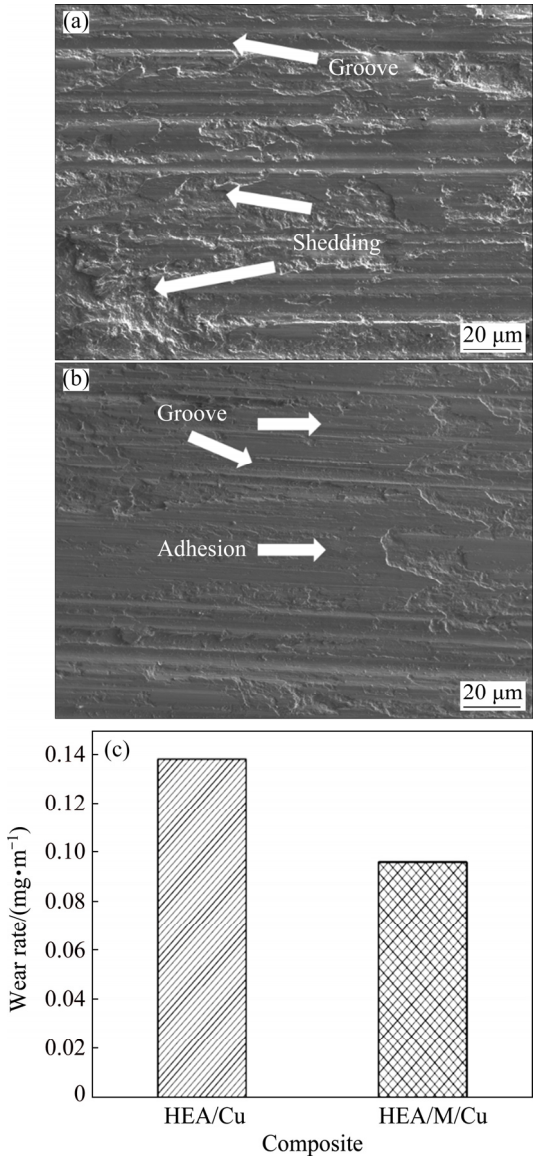

Fig. 11 SEM micrographs of worn surfaces of HEA/Cu (a) and HEA/M/Cu (b) composites and wear rate of two composites (c)

4 Discussion

4.1 Mechanical alloying of HEA particles

Powder particles are usually subjected to high energy collision during mechanical alloying, which results in cold welding among the particles [24−27]. A process of repeated cold welding and fracturing of particles causes the formation of clean surfaces with minimized diffusion distance. Laminated structure is obtained at the initial stage of the MA process, but the chemical composition of the whole particles varies significantly. A characteristic layered structure consisting of many welded small particles is observed during the HEA milling [27]. Then, more refined and complexed multilayer structures are induced due to the repeated fracturing of particles. Owing to a large number of

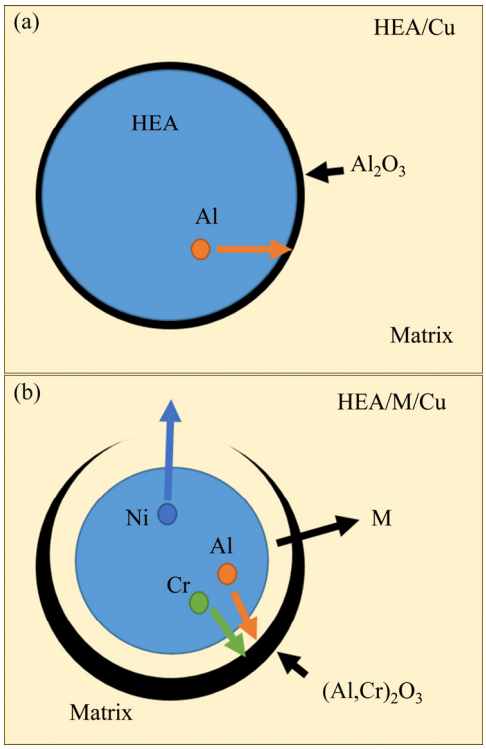

Fig. 12 Schematic diagrams of effect of transition layer structure on elemental diffusion during sintering: (a) HEA/Cu composites; (b) HEA/M/Cu composites

defects and free surfaces induced during the MA process, the activation energy is decreased, which is positive for the homogeneous diffusion even at a low temperature for the increase of diffusivity. The decrease of activation energy is critical to diffuse and dissolve among the elements, since the temperatures during MA are usually far from the diffusion temperature [26]. At the final stage, diffusion and dissolution constantly take place, and a homogenous chemical composition is achieved after the long time milling process. Many works have reported that a solid solution of HEA particles was prepared with the pure elements via mechanical alloying [28−34], with ultrafine grain and excellent hardness and strength after the sintering [35]. As shown in Fig. 2, the XRD pattern of HEA particles indicates a single FCC phase obtained via MA for 48 h.

4.2 Effects of transition layer on diffusion behavior

After the fabrication of HEA particles, a new layered structure has been prepared by the MA. A new and clean interface has been generated between the HEA particles and layered structure, which is beneficial to the diffusion of elements of HEAs particles towards the matrix. More Ni diffuses into the matrix than Co and Fe, as shown in Table 1. In the HEA/Cu composite, Cr element of HEA particles is evenly distributed for lack of clean interface between HEA particles and Cu matrix. However, in the HEA/M/Cu composite, Cr element seems to diffuse into alumina coating, and the mixed oxide layer of $(Al,Cr)_2O_3$ is formed, which is similar to the reported experimental results [36,37]. The diffusion of Cr and Fe into an alumina coating applied to Inconel 718 was investigated by DRESSLER et al [36], and the results indicate that many Cr and minor Fe are incorporated into the alumina coating during heat treatment. Cr is used as an active and interface-modified element to prepare Al_2O_3−W composites [37]. The diffusion rate and thickness of Cr in Al_2O_3 are obviously higher than those of Cr in W during sintering. In this work, minor Cr still exists at the interface of HEA/Cu composites, indicating that the diffusion is sluggish. And Cu transition layer provides road and accelerates the diffusion of Cr towards the interface of HEA/M/Cu composites.

5 Conclusions

(1) The $Al_{0.3}CoCrFeNi$ HEA particles with FCC structure are prepared by mechanical alloying. And a new layered structure of HEA particles coated by Cu has been prepared by the MA for 8 h milling, which exhibits two kinds of FCC phases, corresponding to Cu and HEA phase.

(2) In the HEA/Cu composites, component elements of HEA particles are evenly distributed in the particles, except the Al element which is rich at the interface. However, in the HEA/M/Cu composites, a new and clean transition layer (about 5 μm) has been generated. More Cr is diffused into the interface, which forms the complex oxide. Because of the structure of Cu transition layer, the diffusion rates of Ni, Co and Fe elements increase, especially the Ni element.

(3) The wear resistance of HEA/M/Cu composites is better than that of HEA/Cu composites, which is owing to the improvement of interface bonding strength and increase of matrix hardness. The transition layer structure changes the diffusion behavior of elements and wear behavior owing to the new and clean interface via multi-step ball milling. New HEA particles with higher hardness should be chosen to improve the wear resistance in future. This method is potential and applicable for the development of advanced HEA reinforced metallic matrix composites.

References

[1] GU J, ZHANG X, QIU Y, GU M. Damping behaviors of magnesium matrix composites reinforced with Cu-coated and uncoated SiC particulates [J]. Composites Science and Technology, 2005, 65(11−12): 1736−1742.

[2] TSAI P C, JENG Y R. Experimental and numerical investigation into the effect of carbon nanotube buckling on the reinforcement of

CNT/Cu composites [J]. Composites Science and Technology, 2013, 79: 28−34.

[3] NALEPKA K, SZTWIERTNIA K, NALEPKA P. Preferred orientation relationships at the Cu/α-Al_2O_3 interface: Identification and theoretical explanation [J]. Acta Materialia, 2016, 104: 156−165.

[4] PAK J H, KIM G N, HWANG S G, KIM B S, NOH J P, HUH S C. Mechanical properties of Cu matrix composite fabricated by extrusion process [J]. Transactions of Nonferrous Metals Society of China, 2016, 26(10): 2679−2686.

[5] PRAKASH K S, THANKACHAN T, RADHAKRISHNAN R. Parametric optimization of dry sliding wear loss of copper–MWCNT composites [J]. Transactions of Nonferrous Metals Society of China, 2017, 27(3): 627−637.

[6] MOAZAMI-GOUDARZI M, NEMATI A. Tribological behavior of self lubricating Cu/MoS_2 composites fabricated by powder metallurgy [J]. Transactions of Nonferrous Metals Society of China, 2018, 28(5): 946−956.

[7] ZHANG X, YAN C, YU Z. In-situ combustion synthesis of ultrafine TiB_2 particles reinforced Cu matrix composite [J]. Journal of Materials Science, 2004, 39(14): 4683−4685.

[8] LUO X, YANG Y, MEI Y, HUANG B, YUAN M, CHEN Y. Titanium interlayers as adhesion promoters for SiC_f/Cu composites [J]. Scripta Materialia, 2007, 56(7): 569−572.

[9] LUO X, YANG Y, LIU C, XU T, YUAN M, HUANG B. The thermal expansion behavior of unidirectional SiC fiber-reinforced Cu-matrix composites [J]. Scripta Materialia, 2008, 58(5): 401−404.

[10] CHO S, KIKUCHI K, MIYAZAKI T, TAKAGI K, KAWASAKI A, TSUKADA T. Multiwalled carbon nanotubes as a contributing reinforcement phase for the improvement of thermal conductivity in copper matrix composites [J]. Scripta Materialia, 2010, 63(4): 375−378.

[11] ZHANG J, HE L, ZHOU Y. Highly conductive and strengthened copper matrix composite reinforced by $Zr_2Al_3C_4$ particulates [J]. Scripta Materialia, 2009, 60(11): 976−979.

[12] YEH J W, CHEN S K, LIN S J, GAN J Y, CHIN T S, SHUN T T, TSAU C H, CHANG S Y. Nanostructured high-entropy alloys with multiple principal elements: Novel alloy design concepts and outcomes [J]. Advanced Engineering Materials, 2004, 6(5): 299−303.

[13] MIRACLE D, SENKOV O. A critical review of high entropy alloys and related concepts [J]. Acta Materialia, 2017, 122: 448−511.

[14] TSAI M H, YEH J W. High-entropy alloys: A critical review [J]. Materials Research Letters, 2014, 2(3): 107−123.

[15] CHUANG M H, TSAI M H, WANG W R, LIN S J, YEH J W. Microstructure and wear behavior of $Al_xCo_{1.5}CrFeNi_{1.5}Ti_y$ high-entropy alloys [J]. Acta Materialia, 2011, 59(16): 6308−6317.

[16] GLUDOVATZ B, HOHENWARTER A, CATOOR D, CHANG E H, GEORGE E P, RITCHIE R O. A fracture-resistant high-entropy alloy for cryogenic applications [J]. Science, 2014, 345(6201): 1153−1158.

[17] CHEN J, NIU P, WEI T, HAO L, LIU Y, WANG X, PENG Y. Fabrication and mechanical properties of AlCoNiCrFe high-entropy alloy particle reinforced Cu matrix composites [J]. Journal of Alloys and Compounds, 2015, 649: 630−634.

[18] KARTHIK G M, PANIKAR S, RAM G D J, KOTTADA R S. Additive manufacturing of an aluminum matrix composite reinforced with nanocrystalline high-entropy alloy particles [J]. Materials Science and Engineering A, 2017, 679: 193−203.

[19] TAN Z, WANG L, XUE Y, ZHANG P, CAO T, CHENG X. High-entropy alloy particle reinforced Al-based amorphous alloy composite with ultrahigh strength prepared by spark plasma sintering [J]. Materials & Design, 2016, 109: 219−226.

[20] WU Z, KANG P C, WU G H, GUO Q, CHEN G Q, JIANG L T. The effect of interface modification on fracture behavior of tungsten fiber reinforced copper matrix composites [J]. Materials Science and Engineering A, 2012, 536: 45−48.

[21] LU K. The future of metals [J]. Science, 2010, 328(5976): 319−320.

[22] FANG T H, LI W L, TAO N R, LU K. Revealing extraordinary intrinsic tensile plasticity in gradient nano-grained copper [J]. Science, 2011, 331(6024): 1587−1590.

[23] QIANG J, TSUCHIYA K, DIAO H, LIAW P K. Vanishing of room-temperature slip avalanches in a face-centered-cubic high-entropy alloy by ultrafine grain formation [J]. Scripta Materialia, 2018, 155: 99−103.

[24] SCHWARZ R B, KOCH C C. Formation of amorphous alloys by the mechanical alloying of crystalline powders of pure metals and powders of intermetallics [J]. Applied Physics Letters, 1986, 49(3): 146−148.

[25] LU L, LAI M O. Formation of new materials in the solid state by mechanical alloying [J]. Materials & Design, 1995, 16(1): 33−39.

[26] LU L, LAI M O, ZHANG S. Diffusion in mechanical alloying [J]. Journal of Materials Processing Technology, 1997, 67(1): 100−104.

[27] JOO S H, KATO H, JANG M J, MOON J, KIM E B, HONG S J, KIM H S. Structure and properties of ultrafine-grained CoCrFeMnNi high-entropy alloys produced by mechanical alloying and spark plasma sintering [J]. Journal of Alloys and Compounds, 2017, 698: 591−604.

[28] VARALAKSHMI S, KAMARAJ M, MURTY B S. Synthesis and characterization of nanocrystalline AlFeTiCrZnCu high entropy solid solution by mechanical alloying [J]. Journal of Alloys and Compounds, 2008, 460(1−2): 253−257.

[29] ZHANG K B, FU Z Y, ZHANG J Y, SHI J, WANG W M, WANG H, WANG Y C, ZHANG Q J. Nanocrystalline CoCrFeNiCuAl high-entropy solid solution synthesized by mechanical alloying [J]. Journal of Alloys and Compounds, 2009, 485(1−2): L31−L34.

[30] VARALAKSHMI S, KAMARAJ M, MURTY B S. Processing and properties of nanocrystalline CuNiCoZnAlTi high entropy alloys by mechanical alloying [J]. Materials Science and Engineering A, 2010, 527(4−5): 1027−1030.

[31] FANG S, CHEN W, FU Z. Microstructure and mechanical properties of twinned $Al_{0.5}CrFeNiCo_{0.3}C_{0.2}$ high entropy alloy processed by mechanical alloying and spark plasma sintering [J]. Materials & Design, 2014, 54: 973−979.

[32] MOHANTY S, GURAO N P, BISWAS K. Sinter ageing of equiatomic $Al_{20}Co_{20}Cu_{20}Zn_{20}Ni_{20}$ high entropy alloy via mechanical alloying [J]. Materials Science and Engineering A, 2014, 617: 211−218.

[33] BALDENEBRO-LOPEZ F J, HERRERA-RAMÍREZ J M, ARREDONDO-REA S P, GÓMEZ-ESPARZA C D, MARTÍNEZ-SÁNCHEZ R. Simultaneous effect of mechanical alloying and arc-melting processes in the microstructure and hardness of an AlCoFeMoNiTi high-entropy alloy [J]. Journal of Alloys and Compounds, 2015, 643(S1): s250−s255.

[34] JI W, WANG W, WANG H, ZHANG J, WANG Y, ZHANG F, FU Z. Alloying behavior and novel properties of CoCrFeNiMn high-entropy alloy fabricated by mechanical alloying and spark plasma sintering [J]. Intermetallics, 2015, 56: 24−27.

[35] FU Z, CHEN W, WEN H, MORGAN S, CHEN F, ZHENG B, ZHOU Y, ZHANG L, LAVERNIA E J. Microstructure and mechanical behavior of a novel $Co_{20}Ni_{20}Fe_{20}Al_{20}Ti_{20}$ alloy fabricated by mechanical alloying and spark plasma sintering [J]. Materials

Science and Engineering A, 2015, 644: 10−16.

[36] DRESSLER M, NOFZ M, DÖRFEL I, SALIWAN-NEUMANN R. Diffusion of Cr, Fe, and Ti ions from Ni-base alloy Inconel-718 into a transition alumina coating [J]. Thin Solid Films, 2012, 520(13): 4344−4349.

[37] JIA L, YANG F, LU Z L, WANG J, LIU P. W−Al_2O_3 heterogeneous bonding by hot-press sintering: Cr diffusion and mechanical strength [J]. Materials Letters, 2018, 211: 216−219.

高熵合金颗粒增强铜基复合材料中基于过渡层结构的元素扩散路径调整

于浩洋[1]，方 伟[1,2]，常若斌[1]，冀璞光[1]，王清周[1]

1. 河北工业大学 材料科学与工程学院 能源装备材料技术研究院，天津 300132；
2. 天津市材料层状复合与界面控制技术重点实验室，天津 300132

摘 要：采用机械合金化和烧结法制备 $Al_{0.3}CoCrFeNi$ 高熵合金(HEA)颗粒增强铜基复合材料(CMCs)。采用多步球磨法获得过渡层结构，研究过渡层结构对铜基复合材料中元素扩散行为和材料磨损性能的影响。结果表明，通过多步球磨法得到厚度约为 5 μm 的新铜过渡层。铬元素通过过渡层扩散到界面中，形成复合氧化物。由于铜过渡层的存在，Ni、Co 和 Fe 的扩散率增大，尤其是 Ni 元素。该方法制备的 CMCs 与无过渡层结构的 CMCs 相比，耐磨性提高了 30%，这是由于界面结合强度得到提高。该方法可用于开发先进的 HEA 增强金属基复合材料。

关键词：高熵合金；铜基复合材料；过渡层结构；扩散；磨损

(Edited by Wei-ping CHEN)